A Contact Mechanics Method for Characterizing the Elastic Properties and Permeability of Gels

CHUNG-YUEN HUI,[1] YU YUN LIN,[2] FU-CHIN CHUANG,[2] KENNETH R. SHULL,[3] WEI-CHUN LIN[3]

[1]Department of Theoretical and Applied Mechanics, Cornell University, Ithaca, New York 14853

[2]Department of Civil Engineering, National Cheng Kung University, Tainan, 701, Taiwan, People's Republic of China

[3]Department of Materials Science and Engineering, Northwestern University, Evanston, Illinois 60208

Received 7 January 2005; revised 14 April 2005; accepted 18 May 2005
DOI: 10.1002/polb.20613
Published online in Wiley InterScience (www.interscience.wiley.com).

ABSTRACT: When a saturated gel immersed in the same liquid is suddenly brought into contact with a smooth rigid indenter, the liquid cannot immediately flow out of the pores, and so the gel initially behaves as an incompressible material. This gives rise to a pressure gradient in the liquid phase and the liquid flows until the pressure in it goes to zero everywhere, and all the stresses are transferred to the elastic network. As a result of the flow, the force needed to maintain a constant contact area relaxes with time. In this work, we study the feasibility of using an indentation test to measure this time-dependent force and to determine the elastic modulus, the Poisson's ratio, and the permeability, D_p, of the network. Specifically, we consider a two-dimensional Hertz contact problem of a rigid circular cylinder indenting on a half space consisting of an elastic gel. The network of the gel is assumed to be linearly elastic and isotropic, and liquid flow within the gel is assumed to obey Darcy's law, which states that the flux is proportional to the pressure gradient. Exact expressions are obtained for the initial and final force required to maintain a given contact length. These expressions allow us to determine the elastic constants of the network. The permeability of the network can be obtained from the time-dependent relaxation of the load, which is obtained by solving the exact continuum equations. ©2005 Wiley Periodicals, Inc. J Polym Sci Part B: Polym Phys 43: 359–370, 2006
Keywords: Darcy's law; elastic gel; indentation; permeability

INTRODUCTION

In a series of articles, Scherer[1,2] has laid down the foundation to analyze the stress and deformation in gels. To determine the stresses in such bodies, Scherer[3] has developed a novel test to measure the elastic and viscoelastic properties, as well as the permeability, of these types of gels. In this test, a simply supported gel beam is loaded by imposing a sudden displacement to its midpoint. With the deflection of the beam held constant, the load relaxes, as the liquid in the gel flows. By modeling the kinetics of beam deformation, Scherer obtained a closed form solution for the relaxation of the load. Using this solution and the experimental load relaxation curve, Scherer successfully determined the Young's modulus and the Poisson's ratio of the drained network, as well as the permeability of these types of aerogels.

The gels used in Scherer's experiments were aerogels with elastic moduli near 10^6 Pa, whereas polymer gels typically have elastic moduli in the range of 10^3–10^4 Pa. The beam-bending test is

Correspondence to: C.-Y. Hui (E-mail: ch45@cornell.edu)
Journal of Polymer Science: Part B: Polymer Physics, Vol. 43, 359–370 (2006)

difficult to be applied to materials with these low elastic moduli, for two reasons. First, the beams are difficult to handle because they deform under their own weight and are highly sensitive to adhesive interactions with other materials with which they come into contact. The second reason is connected with the timescale of the pressure-driven flow responsible for the stress relaxation. The driving force for fluid flow scales with the elastic modulus of the material. As a result, the stress relaxation time for materials with similar pore size distributions will scale inversely with the elastic modulus. The effective pore size in a homogeneous polymer gel is the hydrodynamic screening length.[4] This length depends on polymer concentration, but is generally in the nanometer range and is comparable to the characteristic pore size in the gels investigated by Scherer. Small samples are therefore needed to be used for the relaxation times associated with the fluid flow to be experimentally accessible, a fact that further increases the relative importance of adhesive interactions.

Indentation tests have been extremely useful for characterizing the adhesive properties of soft materials.[5–8] In this work, we present a theoretical study of an indentation test designed to determine the elastic properties and permeability of elastic gels. Our specific focus is on a geometry that was employed by Chaudhury et al.[9] to study the surface energy of polydimethylsiloxane (PDMS) because an analytic solution can be developed in this case. The geometry is shown in Figure 1. A rigid circular cylinder of radius R is brought into contact with a half space composed of gel. The length of the indenter, L, is assumed to be very long in comparison with its radius, R. In practice, it is sufficient to have $L/R \approx 50$. The gel occupies the lower half space $x_2 \equiv y < 0$ and the undeformed surface of the gel is the x_1x_2 plane. At time $t = 0$, a sudden displacement is applied to the indenter. This results in a rectangular contact strip of length L and width $2a$. The contact strip width is assumed to be much less than R. In practice, it is sufficient to have $a/R \leq 0.1$. The origin $x_1 = x_2 = x_3 = 0$ is the center of the contact strip. Let $F(t)$ denote the force per unit length of the cylinder needed to maintain a constant contact length $2a$. Our goal is to determine $F(t)$ and to relate $F(t)$ to the elastic constants and permeability of the gel. To do this, we have to solve the time-dependent stress and deformation fields in the gel. In this article, we assume that there are no adhesive forces between the gel and the indenter, although the treatment can be generalized to include adhesive forces.

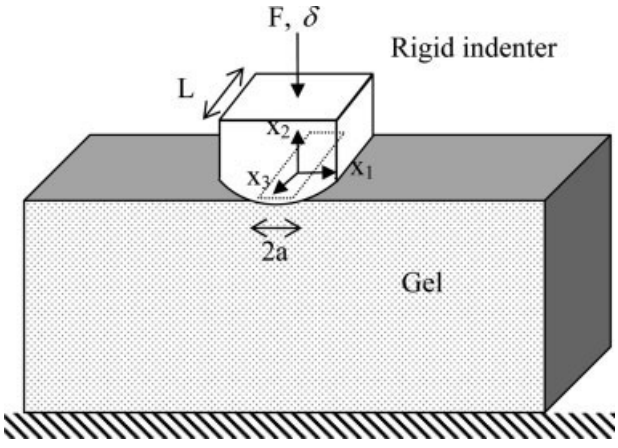

Figure 1. The geometry of the two-dimensional indentation test of a gel. The length, L, of the cylindrical punch is much greater than the contact width, $2a$.

SUMMARY OF FIELD EQUATIONS

The use of a full three-dimensional constitutive model to analyze the quasi-static deformation of elastic gels is first due to Scherer.[1–3] Scherer's model is actually a special case of a model proposed earlier by Biot,[10] who was interested in quasi-static fluid flow in a porous media—an area of particular interest to civil and environmental engineers. Interested readers are referred to the articles by Rice and Cleary[11] and Chandler and Johnson.[12] For wave propagation in gels, readers are referred to the articles by Biot[13] and Johnson.[14] Because the full formulation of governing equations for quasi-static deformation in three dimensions has not appeared in the gel literature, a brief summary is given here. Details can be found in articles by Rice and Cleary,[11] Biot,[10] and Wang.[15]

In Scherer's model, the strain tensor ε_{ij} is related to the stress tensor σ_{ij} and the fluid pressure P by:

$$\varepsilon_{\alpha\beta} = \frac{(1+\upsilon)}{E}\,\sigma_{\alpha\beta} - \frac{\upsilon\sigma_{\gamma\gamma}}{E}\,\delta_{\alpha\beta} - \frac{P}{3K}\,\delta_{\alpha\beta} \qquad (1)$$

where E and υ are the Young's modulus and the Poisson's ratio of the drained network. In this work, the summation convention of summing

over repeated indices is used throughout. We have also used the convention of Scherer where a positive pore pressure corresponds to hydrostatic tension. The bulk modulus of the drain network, K, is related to E and v by:

$$K = \frac{E}{3(1-2v)} \tag{2}$$

The shear modulus of the gel is

$$G = \frac{E}{2(1+v)} \tag{3}$$

It should be noted that, due to the pore pressure term, the constitutive model (1) is no longer that of an isotropic linear elastic solid. Equation 1 assumes that the solid and the liquid phases are both incompressible, which is a good approximation because of the much higher compressibility of the network. Let the position of a material point in the gel be denoted by x_α, $\alpha = 1,2,3$. The stress tensor, $\sigma_{\alpha\beta}$, in the absence of body forces and ignoring inertia, satisfies the equilibrium equations

$$\sigma_{\alpha\beta,\beta} = 0 \tag{4}$$

where a comma denotes partial derivative with respect to x_α.

The pore pressure P is related to the flux of the gel liquid, J_α, by Darcy's law,[1,10] *i.e.*,

$$J_\alpha = D_p P_{,\alpha}/\eta \tag{5}$$

where D_p is the permeability and η is the viscosity of the pore fluid. Mass conservation and the incompressibility of the solid and liquid phases imply that

$$\frac{\partial \varepsilon_{\alpha\alpha}}{\partial t} = -J_{\alpha,\alpha} \tag{6}$$

Equations 1, 5, and 6, and the stress compatibility equations can be used to obtain[11]

$$\nabla^2\left[\sigma_{\alpha\alpha} - \frac{2(1-2v)}{(1-v)}P\right] = 0 \tag{7}$$

That is, $\sigma_{\alpha\alpha} - \frac{2(1-2v)}{(1-v)}P$ is a harmonic function of the spatial variables. Equation 7 shows that the pore pressure field is, in general, coupled to the hydrostatic deformation of the gel.

For many problems of interest, it is advantageous to treat the pore pressure as a body force field in "fictitious" linear elastic body with the same geometry and the same modulus E and Poisson's ratio v. To understand the idea behind this method, rewrite eq 1 as

$$2G\varepsilon_{\alpha\beta} + \lambda\varepsilon_{\gamma\gamma}\,\delta_{\alpha\beta} = \sigma_{\alpha\beta} - P\delta_{\alpha\beta} \tag{8}$$

where $\lambda = \frac{Ev}{(1+v)(1-2v)}$. One can then define an effective stress field, σ^f_{ij}

$$\sigma^f_{\alpha\beta} = \sigma_{\alpha\beta} - P\delta_{\alpha\beta} \tag{9}$$

Equation 8 implies that the effective stress is related to the strain of the gel by the constitutive model of an isotropic linearly elastic solid. In addition, since ε_{ij} is the actual deformation field of the gel, the effective stress field satisfies the stress compatibility equations. Combining eqs 4 and 9 gives:

$$\sigma^f_{\alpha\beta,\beta} = -P_{,\alpha} \tag{10}$$

Equation 10 is the equilibrium equation in a body subjected to distributed body forces $P_{,\alpha}$. Equations 8–10 imply that if the fluid pressure field is known, then the solution of any gel problem can be reduced to solving the problem of a linear elastic body with the same geometry acted on by distributed body forces $P_{,\alpha}$.

The boundary conditions in the "fictitious" elasticity problem with body force can be different from the original. For example, suppose the surface traction T_α is prescribed on part of the boundary of the gel, denoted by $\partial\Omega_T$,

$$\sigma_{\alpha\beta}\,n_\beta = T_\alpha \quad \text{in } \partial\Omega_T \tag{11}$$

where n_β is the outward normal to $\partial\Omega_T$. In the "fictitious" problem, this boundary condition must be replaced by (using eq 9)

$$\sigma^f_{\alpha\beta}\,n_\beta = T_\alpha - Pn_\alpha \quad \text{in } \partial\Omega_T \tag{12}$$

On the other hand, since the displacement field in the modified problem is the actual displacement field, the displacement boundary conditions remains unchanged. Of course, after solving the fictitious body problem, the pore pressure must be added to the effective stress field, to obtain the actual stress in the body. Finally, Biot[10] showed that the dilational strain satisfies

$$D_c\nabla^2\varepsilon_{\alpha\alpha} = \partial\varepsilon_{\alpha\alpha}/\partial t \tag{13a}$$

with

$$D_c = E_l D_p/\eta \tag{13b}$$

and

$$E_l = E(1-v)[(1-2v)(1+v)]^{-1} = K + \frac{4G}{3} \tag{13c}$$

Here, E_l is the longitudinal elastic modulus obtained, for example, from an experiment in which the gel is compressed uniaxially while maintaining a constant cross-sectional area. Note that for a homogeneous gel, D_c is the cooperative diffusion coefficient that is measured in a light-scattering experiment.[16] Equation 13a can be written in terms of the effective pressure $\sigma^f_{\alpha\alpha}$ as

$$D_c \nabla^2 \sigma^f_{\alpha\alpha} = \partial \sigma^f_{\alpha\alpha}/\partial t \tag{13d}$$

While pressure-driven flow is not truly a diffusive process, eq 13d can be viewed as a diffusion equation for the effective pressure.

The following result is an immediate consequence of the governing equations: if a sudden load or displacement is imposed on an initially stress-free gel body at $t = 0^+$, then

$$P(t=0^+) = \frac{\sigma_{\alpha\alpha}(t=0^+)}{3} \tag{14}$$

Equation 14 is a consequence of eq 8 and the fact that diffusion of pore fluid takes finite time; thus, at the instant of load application, the gel behaves as an incompressible linear elastic material. Indeed, if we substitute eq 14 into eq 1, the behavior of the gel, right at the instant of loading, is:

$$\varepsilon_{\alpha\beta}(0^+) = 2G\left(\sigma_{\alpha\beta}(0^+) - \frac{\sigma_{\gamma\gamma}(0^+)}{3}\,\delta_{\alpha\beta}\right) \tag{15}$$

GOVERNING EQUATIONS FOR PLANE STRAIN DEFORMATION

Equations 1–15 are valid for general deformations in three dimensions. In this section, we consider an important class of deformation called plane strain deformation, where the out-of-plane displacement is constant and the in-plane displacements are functions only of the in-plane coordinates x_i, $i = 1,2$ and time t. Indeed, since the length of the rigid cylinder is much greater than the contact width, the deformation of the gel is well approximated by plane strain deformation. Since the problem is two-dimensional, the subscripts will be denoted by i and j instead of the Greek symbols α and β. Also, for convenience, we will also use the notation $x_1 = x$ and $x_2 = y$ in scalar equations.

Using the definition of plane strain, the constitutive model (1) reduces to:

$$2G\varepsilon_{ij} = \sigma_{ij} - v\sigma_{kk}\,\delta_{ij} - (1-2v)\,P\delta_{ij}, \tag{16}$$

Equation 7 reduces to

$$\Delta(\sigma_{kk} - 2\omega P) = 0, \tag{17}$$

where $\omega = (1-2v)/[2(1-v)]$ and Δ is the Laplacian in two dimensions. Equation 17 implies that $\sigma_{kk} - 2\omega P$ is the real part of an analytic function Φ, *i.e.*,

$$4\,\mathrm{Re}\,\Phi = \sigma_{kk} - 2\omega P = \frac{\sigma_{kk}}{2(1-v)} + \omega\sigma^f_{kk} \tag{18}$$

where $\sigma^f_{kk} = (\sigma_{kk} - 2P)$ is the effective hydrostatic tension in 2D. For the case of plane strain, the initial pressure P_0 due to a sudden load is:

$$P_0 = \sigma_{kk}(t=0^+)/2 \tag{19}$$

Finally, eq 13c reduces to

$$\partial \sigma^f_{kk}/\partial t = D_c\,\Delta\sigma^f_{kk}, \tag{20}$$

or using eq 18

$$D_c \Delta P = \partial P/\partial t - 4(1-v)\,\mathrm{Re}(\partial\Phi/\partial t) \tag{21}$$

As pointed out by Rice and Cleary,[11] eq 21 implies that the pressure distribution is decoupled from the stress fields, provided that Φ is time independent.

The plane-strain equations developed can now be applied to our specific geometry illustrated in Figure 1. The relationship between the contact width and the normal displacement for a rigid, curved indenter is purely geometrical, and does not depend on the elastic properties of the material with which it comes into contact. For an elastic half space ($h = \infty$), the following relationship is obtained[17]

$$\delta = \frac{a^2}{4R}\{2\ln(4R/a) - 1\} \tag{22}$$

An important consequence of eq 22 is that the contact width is determined by the applied dis-

placement, and is independent of the elastic properties of the gel. The load relaxation, which occurs as a result of the solvent flow, therefore, occurs at a fixed value of a, provided that the displacement δ is maintained at a constant value during the experiment.

The assumed protocol for a load relaxation experiment involves a rapid increase in the displacement, over a timescale that is short enough so that redistribution of the stress due to solvent flow is negligible. The short- and long-time solutions for the load and displacement can be obtained by considering results obtained for the indentation of a material with an effective Poisson's ratio, v_{eff}, which is equal to 0.5 at short times, and decays to v, Poisson's ratio of the drained gel, at long times. The appropriate expression for the force is:

$$F = \frac{\pi G a^2}{2R\,(1 - v_{\text{eff}})}. \tag{23}$$

Similarly, the hydrostatic stress distribution in the gel is given by the following expression from Muskhelishvili[18]:

$$\sigma_{kk}(y,z) = \frac{G}{R(1 - v_{\text{eff}})}\left(\sqrt{a^2 - z^2} + \overline{\sqrt{a^2 - z^2}} - 2y\right), \tag{24}$$

where $z = x + iy$, $i = \sqrt{-1}$.

At $t = 0^+$, the gel behaves as an incompressible solid with $v_{\text{eff}} = 0.5$. The initial pore pressure is obtained from eq 24 as:

$$P_0 \equiv \sigma_{kk}(z, t \to 0^+)/2 = \frac{G}{R}\,\text{Re}\left(\sqrt{a^2 - z^2} + \overline{\sqrt{a^2 - z^2}} - 2y\right) \tag{25}$$

The corresponding initial load $F(t = 0^+)$ required for contact (with contact length a) is:

$$F_0 \equiv F(t \to 0^+) = \pi G a^2/R \tag{26}$$

At long times, the pore pressure reduces to zero ($P_\infty \equiv P\,(t \to \infty) = 0$), σ_{kk} in the gel is,

$$\sigma_{kk}(z, t \to \infty) = \frac{G}{R(1 - v)} \times \text{Re}\left(\sqrt{a^2 - z^2} + \overline{\sqrt{a^2 - z^2}} - 2y\right) \tag{27a}$$

and the force is obtained by setting v_{eff} to v:

$$F_\infty \equiv F(t \to \infty) = \frac{\pi G a^2}{2R\,(1 - v)} \tag{27b}$$

Equations 26 and 27 enable the shear modulus and the Poisson's ratio to be determined from the short time and long time force data. Note that the fractional load relaxation depends only on the Poisson's ratio, that is:

$$\frac{F_\infty}{F_0} = \frac{1}{2(1 - v)}, \quad \frac{F_0 - F_\infty}{F_0} = \omega = \frac{1 - 2v}{2(1 - v)} \tag{28}$$

Using eqs 18, 25, and 27a, it is easy to show that Re $\Phi(z, t \to 0^+)$ = Re $\Phi(z, t \to \infty)$. Physically, we anticipate that σ_{kk} and $-P$ are monotonically decreasing functions of time. This implies that Re Φ is also a monotonically decreasing function of time. Since Re $\Phi(z, t \to 0^+)$ = Re $\Phi(z, t \to \infty)$, Re Φ is time independent and the pressure field is decoupled form the stresses. This result is also justified by our recent finite element analysis, which solved the full coupled problem. The force *versus* time result of our finite element solution is in good agreement with the results of this work.

Determination of the Cooperative Diffusion Coefficient

The cooperative diffusion coefficient D_c can be determined from the kinetics of load relaxation; this requires the solution of all the field equations, not just the asymptotic behavior of the load. The quantity of interest is the force on the indenter as a function of time. This force can be computed using the normal stress field σ_{22} (x, $y = 0$, t), *i.e.*,

$$F(t) = -\int_{-a}^{a} \sigma_{22}(x, y = 0, t)\,dx \tag{29a}$$

By, eq 9, $\sigma_{22} = \sigma_{22}^f + P$, so

$$F(t) = -\int_{-a}^{a} \sigma_{22}^f(x, y = 0, t)\,dx - \int_{-a}^{a} P(x, y = 0, t)\,dx \tag{29b}$$

Because the solution of these two problems is very complicated, we give the details in the appendixes. In the following, we summarize the procedures and results.

Since the stresses are decoupled from the pore pressure, the solution can be obtained in two steps. In step one, we solve for the pore pressure using eq 21, with $\partial\ \mathrm{Re}\ \Phi/\partial t = 0$ subjected to the following boundary conditions:

$$P(|x| > a, t > 0) = 0 \tag{30a}$$

$$P_{,2}(|x| < a, y = 0^-, t > 0) = 0 \tag{30b}$$

The initial condition is given by eq 25, *i.e.*,

$$P(x, y < 0, t = 0^+) = \frac{G}{R}\left(\sqrt{a^2 - z^2} + \overline{\sqrt{a^2 - z^2}} - 2y\right) \tag{30c}$$

The method of solution of the fluid pressure is given in Appendix A. It is interesting to note that the gradient of the pressure field has a square root singularity at the edge of contact. Specifically, the behavior of the pressure gradient near the contact edge has the following form

$$\begin{aligned} P_{,1} &= -A(t)\rho^{-1/2}\sin(\theta/2), \\ P_{,2} &= A(t)\rho^{-1/2}\cos(\theta/2) \end{aligned} \qquad \rho \to 0 \tag{31}$$

where $(\rho,\ \theta)$ is a local polar coordinate system with origin at $z = a$, *i.e.*, $z - a = \rho e^{i\theta}$.

In step two, the fluid pressure obtained in step one is treated as a body force field in "fictitious" linear elastic body with Young's modulus E and Poisson's ratio v (see eq 10). The stresses of the "fictitious" body are denoted by σ^f_{ij}. Specifically, we solve the Hertz problem of a cylindrical rigid indenter indenting on a half space subjected to time-dependent body forces $P_{,i}$, which is obtained from step one. It turns out for any body force field, an exact closed form solution can be found for the Hertz problem. This result allows us to compute the time history of the indentation force $F(t)$, which is found to be:

$$F(t) = F_\infty + 4a^2\frac{\kappa - 1}{\kappa + 1} \times \int_{-\infty}^{0}\int_{0}^{\infty} P(x', y')\ \mathrm{Im}\left(\frac{\chi(s)}{(s^2 - a^2)}\right) dx'\, dy' \tag{32a}$$

where F_∞ is given by eq 27 and

$$\chi(s) = 1/\sqrt{s^2 - a^2} \tag{32b}$$

$$s = x' + iy' \tag{32c}$$

$$\kappa = 3 - 4v \tag{32d}$$

The derivation of eqs 32a–d is given in Appendix B.

NORMALIZATION

The following normalized variables are used to expedite the analysis and to gain physical insight. All distances are normalized by the contact length a. From dimensional analysis, the pore pressure and stresses must scale with Ga/R and time scales with a^2/D_c. Thus, the normalized distances are $\eta = x/a$, $\xi = y/a$; the normalized pore pressure is $\varphi = \frac{RP}{Ga}$; the normalized load is $\bar{F} = \frac{R}{\pi Ga^2}F$; and the normalized time is $\tau = D_c t/a^2$. The characteristic load relaxation time is therefore of order a^2/D_c. The coupling of the timescale to the size of the contact zone provides a means for experimentally distinguishing between load relaxation resulting from solvent flow and load relaxation resulting from viscoelastic relaxation of the gel network, since viscoelastic effects are independent of the contact width. Using these normalizations, it can be shown that the normalized field equations and the boundary conditions depends only on the Poisson's ratio, so that a plot of $\bar{F} = \frac{R}{\pi Ga^2}F$ *versus* $\tau = D_c t/a^2$ is independent of geometry (*e.g.*, the amount of contact, the radius of curvature of the indenter) and material properties, with the exception of the Poisson's ratio v. According to eqs 26 and 27, the short and long time behavior of the normalized indenter force is given by

$$\begin{aligned} &\bar{F}(\tau \to 0) = 1, \\ &\bar{F}(\tau \to \infty) = \frac{1}{2(1 - v)} \le 1 \end{aligned} \tag{33}$$

Figure 2 plots the normalized indenter force $\bar{F} = \frac{R}{\pi Ga^2}F$ *versus* the normalized time $\tau = D_c t/a^2$ for Poisson's ratios $v = 0.3$ and 0.25, respectively. The cooperative diffusion coefficient, D_c, can be obtained by comparing the experimentally measured time dependence of the stress relaxation to the predicted relaxation behavior. Figure 3 shows the following fit to the relaxation behavior that is obtained numerically

$$\bar{F} = \frac{1}{2(1 - v)}[1 + (1 - 2v)\Delta\bar{F}] \tag{34a}$$

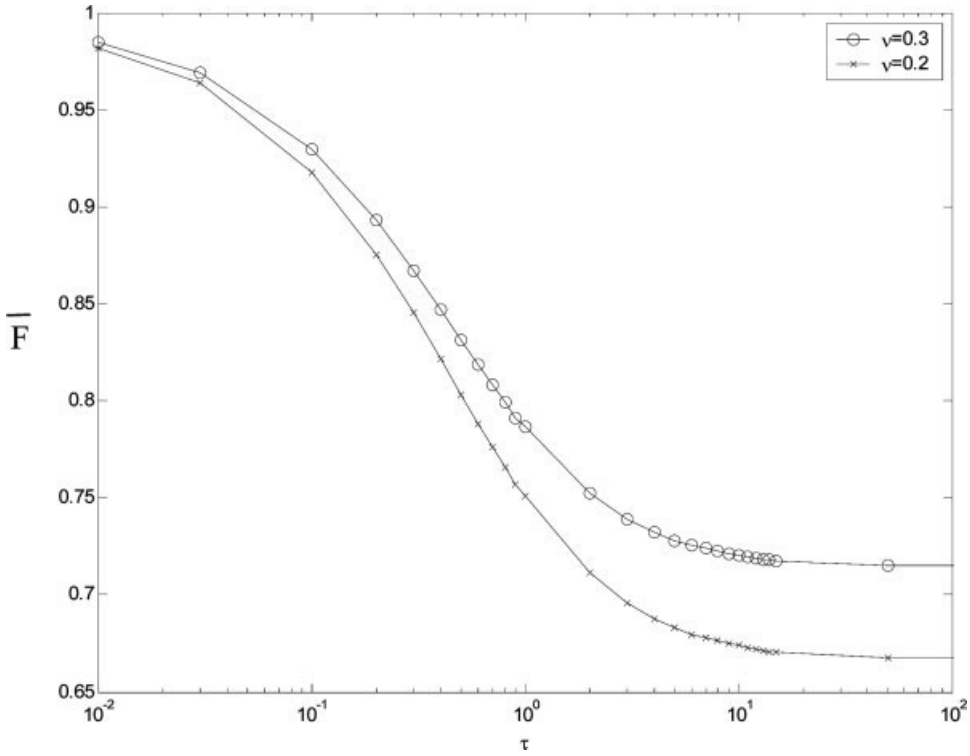

Figure 2. The normalized indenter force $\bar{F} = \frac{R}{\pi G a^2} F$ *versus* the normalized time $\tau = D_c t/a^2$ for Poisson's ratio $v = 0.3$. and $v = 0.25$.

where

$$\Delta\bar{F} = \exp(-\sqrt{0.3\tau} - 2\tau) \tag{34b}$$

Figure 3 shows that eqs 34a,b are valid as long as $\tau < 1$.

SUMMARY AND DISCUSSIONS

Equations 26 and 27 suggested that the initial and final indentation forces measured in experiments can be used to determine the shear modulus and the Poisson's ratio of the drained elastic gel. The characteristic relaxation time of an indentation experiment is of order a^2/D_c. Scherer[3] has shown that, for a silica gel containing ethanol, $v \simeq 0.22$, $E \simeq 3$ MPa, and $D_p \simeq 7.4$ nm^2. The viscosity of ethanol at room temperature is $\eta \simeq 1.1 \times 10^{-3}$ Pa s. This results in $D_c \cong 2.2\times10^{-7}$ m^2/s. Thus, the characteristic relaxation time is on the order of $4.6a^2 \times 10^6$ s. The relaxation time is about 114 s, if the contact width is 5 mm. We emphasize that the gel properties cited earlier are for one particular gel; in general, the elastic moduli and permeabilities of silica gels can vary by an order of magnitude above and below these values.

To make the connection to polymer gels, which are not typically viewed as porous media, it is useful to consider the situation for polymer gels in a good solvent, as described in a series of papers by Geissler and Hecht.[19–26] For polymer gels consisting of a crosslinked polymer in a good solvent, the cooperative diffusion coefficient is related to the hydrodynamic screening length, ξ_h, by the following expression:

$$D_c = \frac{k_B T}{6\pi\eta\xi_h} \tag{35}$$

Geissler et al.,[23] measured D_c for a series of polyacrylamide hydrogels that were swollen to equilibrium in the solvent (water), and obtained values of D_c ranging from 10^{-11} to 5×10^{-11} m^2/s. These values of D_c correspond to values of ξ_h in the range of 4–20 nm, which is quite typical of most homogeneous polymer gels.[4] Values of the longitudinal elastic modulus, E_l, were also obtained by Geissler and Hecht[19,22] from measurements of the absolute scattering intensity. Equation 13b can be used to extract the permeability, which was approximately equal to $0.3\xi_h^2$,

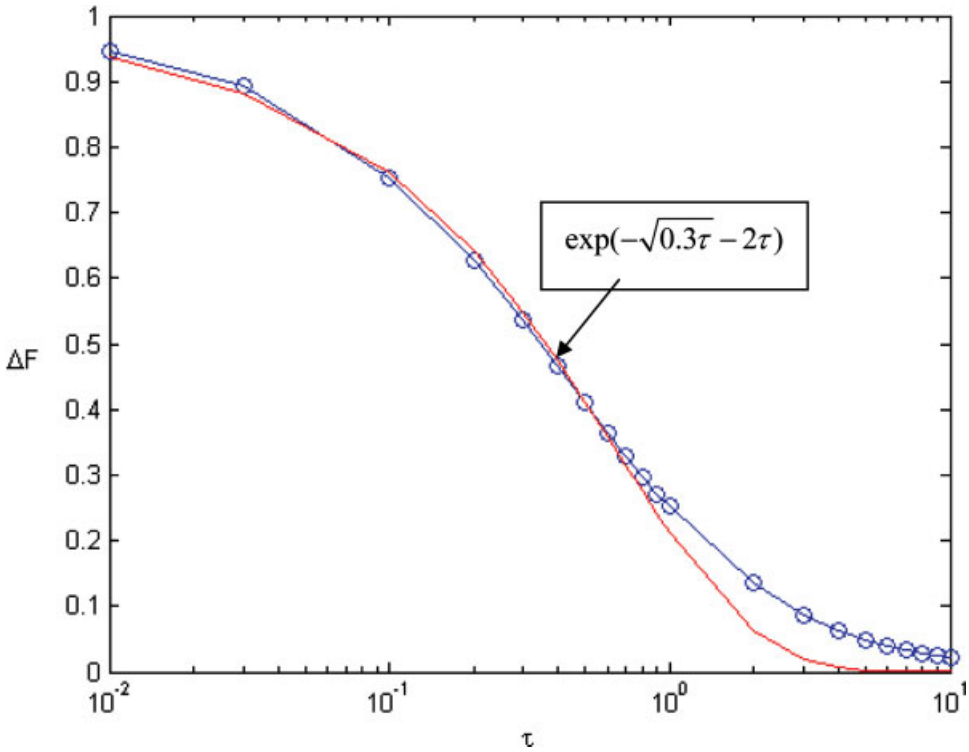

Figure 3. The normalized indenter force $\Delta\bar{F}=\frac{R}{\pi G a^2}(F-F_\infty)$ *versus* the normalized time $\tau = D_c t/a^2$. Red line is plotted by the fitting function $\bar{F}=\frac{1}{2(1-v)}[1+(1-2v)\Delta\bar{F}]$. [Color figure can be viewed in the online issue, which is available at www.interscience.wiley.com.]

and varied between 6 and 50 nm^2. From this, we see that the relevant pore size for these homogeneous gels is the hydrodynamic screening length, which is similar to the pore size of the gels analyzed by Scherer. Values of D_c are much lower for the polymer gels than for Scherer's gels, however, because of the much lower values of E_l. As a result, much smaller sample sizes are needed to use a stress relaxation technique to measure the permeability of a polymer gel. For a gel with $D_c = 10^{-11}$ m^2/s, in contact with a cylindrical indenter, the contact width needs to be limited to 50 μm, for the characteristic relaxation time, a^2/D_c, to be <200 s.

When appropriately analyzed within the context of the theory presented here, measurements of the stress relaxation can be used to determine the permeability and compressibility of the gel. For a homogeneous gel, the permeability is related to the hydrodynamic screen length, and the compressibility corresponds to the osmotic compressibility of the gel. In this case, contact experiments provide a potentially simpler means of determining the same information that can be obtained by independent measurements of the shear modulus, longitudinal elastic modulus, and cooperative diffusion coefficient. The fractional relaxation due to solvent flow can be quite large in polymer gels, which can have relaxed Poisson's ratios of 0.25 or below.[24] A variety of other situations exist, however, where the contact methodology is the only means by which useful information can be obtained. Consider for example, hydrogels based on poly(*n*-isopropylacrylamide) that undergo a phase separation when heated. By controlling the detailed chemistry of these gels, it is possible to produce gels that stiffen considerably when heated through the transition temperature, but which maintain a constant macroscopic volume.[24] These stiffened gels are no longer homogeneous, but consist of polymer-rich and solvent-rich regions. Very little is known about the pore structure in these types of gels, despite their potential importance in a variety of tissue engineering applications. The contact methodology that we are developing is ideally suited for characterizing the transport properties in these types of materials, which because of their opacity, cannot be investigated with light-scattering techniques.

Finally, it is possible to extend the above analysis to include the effects of adhesion and three-dimensional geometries. For example, the short and long time forces required to indent a circular flat punch of radius a on a half space of gel by a fixed distance δ can be founded using Boussinseq's solution.[17] The initial force $F_0 = 8Ga\delta$ will eventually relax to $F_\infty = 4Ga\delta/(1 - v)$ at long times. If the flat punch is replaced by a punch with a hemispherical indenter with radius R and if the radius of the contact circle is maintained at a constant radius a, then it is easy to show that the initial force is $F_0 = \pi Ga^2/R$. At long time, this initial force will relax to $F_\infty = \pi Ga^2/2(1 - v)R$. It is interesting to note that, although the geometries are different (circular indenter in 2D, flat punch in 3D, hemispherical punch in 3D), the ratio of the final force to the initial force is the same, and is $1/[2(1 - v)]$. In both cases (flat punch and hemispherical punch), the pore pressure field will be coupled with the stress field and numerical methods such as finite element method must be used to solve these coupled equations.

Support to K. Shull, from the National Science Foundation (DMR-0214146), and to W. Lin, in the form of a National Physical Science Consortium Fellowship, are gratefully acknowledged. Y.Y. Lin and F.-C. Chuang are supported by the National Science Council in Taiwan (NSC93-2211-E006-069). Discussions with Philip Cole and John Emerson of Sandia National Laboratory are acknowledged.

APPENDIX A: SOLUTION OF THE PORE PRESSURE FIELD

Equation 21 and the initial and boundary conditions, eqs 22 and 33, in normalized form, are:

$$\nabla^2\varphi = \frac{\partial\varphi}{\partial\tau} \tag{A1a}$$

$$\varphi(|\eta| > 1, \tau > 0) = 0 \tag{A1b}$$

$$\frac{\partial\varphi}{\partial\xi}(|\eta| < 1, \xi = 0^-, \tau > 0) = 0 \tag{A1c}$$

$$\varphi(\eta, \xi, \tau = 0^+) = \mathrm{Re}\left(\sqrt{1 - Z^2} + \overline{\sqrt{1 - Z^2}} - 2\xi\right) \equiv \varphi_0 \tag{A1d}$$

where $Z = \eta + i\xi$ and φ_0 is the initial normalized pore pressure field. Let $\phi \equiv \varphi - \varphi_0$, this change of variable implies that initial condition for ϕ is identically zero, *i.e.*, $\phi(\eta, \xi, \tau = 0^+) = 0$. Note that $\phi = \frac{R}{Ga}(P - P(Z, t = 0^+))$ is the normalized difference between the current and initial pore pressure field. Since the initial pore pressure field is harmonic, the governing PDE is unchanged, *i.e.*,

$$\nabla^2\phi = \frac{\partial\phi}{\partial\tau} \tag{A2a}$$

In addition, since the initial pressure field satisfies the boundary condition A1b, the only boundary condition we need to change is A1c. A straight forward calculation shows that the new boundary conditions are

$$\phi(|\eta| > 1, \tau > 0) = 0 \tag{A2b}$$

$$\frac{\partial\phi}{\partial\xi}(|\eta| < 1, \xi = 0^-, \tau > 0) = 2 \tag{A2c}$$

A finite element simulation is carried out to solve the diffusion problem specified by A2a–c.

APPENDIX B: SOLUTION OF THE FICTITIOUS HERTZ CONTACT PROBLEM WITH BODY FORCE $P_{,i}$

The fictitious stress field can be decomposed into

$$\sigma_{ij}^f = \sigma_{ij}^\infty + \sigma_{ij}^* \tag{A3}$$

where σ_{ij}^∞ is the time independent long time Hertz solution (see eqs 24 and 25) where the pore pressure is identically zero everywhere and σ_{ij}^* satisfies the equation

$$\sigma_{ijj}^* = -P_{,i} \tag{A4}$$

Combining A3 and eq 9 gives:

$$F(t) = F_\infty + F^* - \int_{-a}^{a} P(x, y = 0, t)\, dx \tag{A5}$$

where

$$F_\infty = -\int_a^a \sigma_{22}^\infty(x, y = 0, t)\, dx \tag{A6a}$$

$$F^* = -\int_{-a}^{a} \sigma_{22}^*(x, y = 0, t)\, dx \tag{A6b}$$

is given by eq 30. We have thus reduced the problem of determining the indenter force to the problem of determining σ_{ij}^*. Denote the elastostatic fields associated with σ_{ij}^* by (u_i^*, ε_{ij}^*, σ_{ij}^*).

These fields must satisfy the following boundary conditions

$$\sigma_{12}^{*}(|x|>a, y=0, t)=\sigma_{22}^{*}(|x|>a, y=0, t)=0 \tag{A7a}$$

$$\sigma_{12}^{*}(|x|<a, y=0, t)=0 \tag{A7b}$$

$$du_{2}^{*}(|x|<a, y=0, t)/dx=0, \tag{A7c}$$

together with the condition of bounded stresses at the edge of contact. The displacement boundary condition A7c accounts for the fact that the vertical displacement directly underneath the punch is the same as the displacement of displacement of the long time Hertz solution.

Determining σ_{ij}^{*}

The stress and displacements for a linear elastic body under plane strain deformation can be represented by two analytic functions, $\Phi(z)$ and $\Omega(z)$,[18] *i.e.*,

$$\begin{aligned}\sigma_{11}+\sigma_{22}&=4\ \mathrm{Re}\,\Phi(z)\\ \sigma_{22}+i\sigma_{12}&=\overline{\Phi(z)}+\Omega(z)+(\bar{z}-z)\Phi'(z)\\ 2G(u_1+iu_2)_{,1}&=\kappa\Phi(z)-\overline{\Omega(z)}-(z-\bar{z})\overline{\Phi'(z)}\end{aligned} \tag{A8}$$

where $\overline{\Phi(z)}$ denote the complex conjugate of $\Phi(z)$, $\Phi'(z)=d\Phi(z)/dz$, and $\kappa=3-4v$.

The following steps are used to determine σ_{ij}^{*}:

Step 1: Obtain the solution of the following elasticity problem: A concentrated force of magnitude $db(s)=db_1(s)+idb_2(s)$ applied at a point s in the lower half plane. Traction-free boundary conditions are imposed on $y=0$. Denote the stresses and displacements of this problem by $d\sigma_{ij}^{**}$, du_i^{**}. This solution satisfies the boundary conditions A7a,b, but not A7c. The displacement field du_2^{**} on $|x|<a$, $y=0$ is indeed nonzero.

Step 2: Let $db_1(s)=P_{,1}ds_1ds_2$, $db_1(s)=P_{,2}ds_1ds_2$, obtain the stresses at z due to all distributed forces by summing over all s in the lower half plane. The solution of step 2, denoted by σ_{ij}^{**}, u_i^{**} accounts for the distributed forces and satisfies the boundary conditions A7a,b, but not A7c. The displacement field u_2^{**} on $|x|<a$, $y=0$ is indeed nonzero. Note $\sigma_{22}^{**}(x, y=0_-)=0$.

Step 3: Obtain the stresses σ_{ij}^{***} and displacements u_i^{***} of the following elasticity problem: A vertical displacement $u_2^{***}=-u_2^{**}$ is imposed on $|x|<a$, $y=0$. The shear traction is identically zero when $y=0$ and the normal traction is identically zero when $|x|>a$, $y=0$.

Step 4: Add the stresses and displacements obtained in steps 2 and 3; that is let $\sigma_{ij}^{*}=\sigma_{ij}^{**}+\sigma_{ij}^{***}$, $u_i^{*}=u_i^{**}+u_i^{***}$. The resulting fields σ_{ij}^{*}, u_i^{*} is the solution of an elasticity problem with a distributed force $b(s)=P_{,1}(s)+iP_{,1}(s)$ at s. In addition, this solution satisfies the boundary conditions A7a–c.

The solution of step 1 can be found using the method of Muskhelishvili,[18] the potentials $\Phi_1(z)$ and $\Omega_1(z)$ are found to be:

$$\begin{aligned}\Phi_1(z)&=\Phi_0(z)-\overline{\Omega_0(\bar{z})},\\ \Omega_1(z)&=\Omega_0(z)-\overline{\Phi_0(\bar{z})}\end{aligned} \tag{A9a}$$

where

$$\Phi_0(z,s)=-\frac{qdb(s)}{z-s}, \tag{A9b}$$

$$\Omega_0(z,s)=q\frac{\kappa\overline{db(s)}}{z-s}-q\frac{(\bar{s}-s)db(s)}{(z-s)^2} \tag{A9c}$$

$$q=\frac{1}{2\pi(1+\kappa)} \tag{A9d}$$

Using eqs A8 and A9, $du_1^{**}+idu_2^{**}$ is found to be:

$$(du_1^{**}+idu_2^{**})_{,1}=\frac{q(1+\kappa)}{2G}dH(x_1,s,\kappa) \tag{A10a}$$

where

$$dH(x_1,s,\kappa)\equiv\frac{q(1+\kappa)}{2G}\left[-db(s)\left(\frac{\kappa(x_1-s)+(x_1-\bar{s})}{(x_1-s)(x_1-\bar{s})}\right)+\overline{db(s)}\left(\frac{(s-\bar{s})}{(x_1-\bar{s})^2}\right)\right] \tag{A10b}$$

Using eq A10a, the displacement gradient $(u_1^{**}+iu_2^{**})_{,1}$ on $y=0$ is

$$(u_1^{**}+iu_2^{**})_{,1}=\frac{q(1+\kappa)}{2G}\int_{-\infty}^{\infty}dx_1'\int_{-\infty}^{0}H(x,s,\kappa)dy' \tag{A11}$$

where

$$\begin{aligned}s&=x'+iy'\\ H(x,s,\kappa)&\equiv\frac{q(1+\kappa)}{2G}\left[-b(s)\left(\frac{\kappa(x-s)+(x-\bar{s})}{(x-s)(x-\bar{s})}\right)+\overline{b(s)}\left(\frac{(s-\bar{s})}{(x-\bar{s})^2}\right)\right]\\ b(s)&=P_{,1}(s)+iP_{,2}(s)\end{aligned} \tag{A12}$$

The integral A12 converges, since the body forces vanishes as $1/s^2$ as $|s| \to \infty$ therefore, for any fixed x on the interface, $H(x, |s| \to \infty, \kappa) \simeq 1/|s|^3$.

Step 3 is carried out using a result by Muskelishvili.[18] Since our primary interest is the force on the indenter, only the normal stress on $y = 0$ is given here, it is:

$$\sigma_{22}^{***}(x,y=0_-) = \frac{8Gq}{\sqrt{a^2-x^2}} \times \int_{-a}^{a} \frac{\sqrt{a^2-p^2}v'(p)dp}{p-x} + \frac{2D}{\sqrt{a^2-x^2}} \quad \text{(A13a)}$$

where

$$v'(p) = -\frac{1}{4\pi G}\,\mathrm{Im}\left[\int_{-\infty}^{\infty} dx' \int_{-\infty}^{0} H(p,s,\kappa)\,dy'\right] \quad \text{(A13b)}$$

It can be shown that[18]

$$D = -\frac{1}{2\pi}\int_{-a}^{a} \sigma_{22}^{***}(x,y=0_-)\,dx \quad \text{(A13c)}$$

Since σ_{22}^{**} $(x,\ y = 0_-)$ must be bounded at $x = \pm a$, eq A13a implies that[18]

$$D = 4Gq\int_{-a}^{a} \frac{p}{\sqrt{(a+p)(a-p)}} v'(p)\,dp \quad \text{(A13d)}$$

Equations A13b–d imply that

$$-\int_{-a}^{a} \sigma_{22}^{***}(x,y=0_-)dx = -2q\int_{-a}^{a} \frac{p}{\sqrt{(a+p)(a-p)}} \times \mathrm{Im}\left[\int_{-\infty}^{\infty} dx' \int_{-\infty}^{0} H(p,s,\kappa)\,dy'\right] dp \quad \text{(A14)}$$

Step 4: Since σ_{22}^{**} $(x,\ y = 0_-) = 0$, the traction due to step 2 do not contribute to the indenter force. The second term in eq A6 is

$$-\int_{-a}^{a} \sigma_{22}^{*}(x,y=0_-)\,dx \equiv F^* = -2q\int_{-a}^{a} \frac{p}{\sqrt{(a+p)(a-p)}} \times \mathrm{Im}\left[\int_{-\infty}^{\infty} dx' \int_{-\infty}^{0} H(p,s,\kappa)dy'\right] dp \quad \text{(A15)}$$

Equation A15 can be simplified by interchanging the order of integration, thus

$$F^* = -2q\left[\int_{-\infty}^{\infty} dx' \int_{-\infty}^{0} \left(\mathrm{Im}\int_{-a}^{a} \frac{p}{\sqrt{(a+p)(a-p)}} \times H(p,s,\kappa)\,dp\right) dy'\right] \quad \text{(A16)}$$

The integral $I(s) \equiv \int_{-a}^{a} \frac{p}{\sqrt{(a+p)(a-p)}} H(t,s,\kappa)\,dt$ can be evaluated exactly using contour integration. After some tedious calculations, we found

$$I(s) = -b(s)h_1(s) + \overline{b(s)}h_2(s) \quad \text{(A17a)}$$

where

$$h_1(s) = (1+\kappa)\pi - \pi(s\chi(s) + \kappa\bar{s}\chi(\bar{s})) \quad \text{(A17b)}$$

$$h_2(s) = \frac{\pi a^2(s-\bar{s})}{(\bar{s}^2-a^2)}\chi(\bar{s}) \quad \text{(A17c)}$$

$$\chi(s) = \frac{1}{\sqrt{(s-a)(s+a)}} \quad \text{(A17d)}$$

The branch cut of $\chi(s)$ is $[-a,\ a]$ and $\chi(s)$ is computed using the definition:

$$\chi(s) = (r_1 r_2)^{-1/2} e^{-i(\theta_1+\theta_2)/2} \quad \text{(A18a)}$$

where

$$s-a \equiv r_1 e^{i\theta_1}, s+a \equiv r_2 e^{i\theta_2}, -\pi < \theta_1 < \pi, -\pi < \theta_2 < \pi \quad \text{(A18b)}$$

It can be easily shown that

$$F^* = -\frac{1}{\pi(\kappa+1)}\left[\int_{0}^{\infty}\int_{-\infty}^{0} (\mathrm{Im}\,I(-\bar{s}) + \mathrm{Im}\,I(s))\,dy'dx'\right] \quad \text{(A19)}$$

Further simplifications can be achieved using the symmetry conditions,

$$P_{,1}(-\bar{s}) = -P_{,1}(s), \quad P_{,2}(-\bar{s}) = P_{,2}(s), \quad \text{(A20a)}$$

as well as the relations

$$\chi(-s) = -\chi(s), \chi(\bar{s}) = \overline{\chi(s)}, \chi(-\bar{s}) = -\overline{\chi(s)} \quad \text{(A20b)}$$

After some very tedious calculations, we found

$$\mathrm{Im}\,I(-\bar{s}) + \mathrm{Im}\,I(s) = P_1(x',y')f_1(x',y') + P_2(x',y')f_2(x',y') \quad \text{(A20c)}$$

where

$$f_1 = 2(1-\kappa)\pi\ \mathrm{Im}(s\chi(s)) + 4\pi a^2 y'\ \mathrm{Re}\left(\frac{\cdot\chi(s)}{(s^2-a^2)}\right) \quad \text{(A20d)}$$

$$f_2 = -2(1+\kappa)\pi + 2(1+\kappa)\pi\ \mathrm{Re}(s\chi(s))) - 4\pi a^2 y'\ \mathrm{Im}\left(\frac{\chi(s)}{(s^2-a^2)}\right) \quad \text{(A20e)}$$

Combining eqs A19 and A20, we found

$$F^* = -\frac{1}{\pi(\kappa+1)}\left[\int_0^\infty \int_{-\infty}^0 [P_{,1}(x',y')f_1(x',y') + P_{,2}(x',y')f_2(x',y')]\,dy'dx'\right] \quad \text{(A21)}$$

Equation A21 can be further simplified using the divergence theorem. After some tedious calculations, the result is

$$F^* = \int_{-a}^{a} P(x',y=0^-)\,dx' + 4a^2\,\frac{\kappa-1}{\kappa+1} \times \int_{-\infty}^0 \int_0^\infty P(x',y')\ \mathrm{Im}\left(\frac{\chi(s)}{(s^2-a^2)}\right)dx'dy' \quad \text{(A22)}$$

Calculation of the Indenter Force

The indenter force can be computed using eq A22 and eq 27b, *i.e.*,

$$F(t) = F_\infty + F^* - \int_{-a}^{a} P(x,y=0^-)\,dx = F_\infty + 4a^2\frac{\kappa-1}{\kappa+1} \times \int_{-\infty}^0 \int_0^\infty P(x',y')\,\mathrm{Im}\left(\frac{\chi(s)}{(s^2-a^2)}\right)dx'\,dy'. \quad \text{(A23)}$$

REFERENCES AND NOTES

1. Scherer, G. W. J Non-Cryst Solids 1989, 109, 171.
2. Scherer, G. W. J Non-Cryst Solids 1989, 113, 107.
3. Scherer, G.W. J Non-Cryst Solids 1992, 142, 18.
4. Adam, M.; Delsanti, M. Macromolecules 1977, 10, 1229.
5. Lakrout, H.; Creton, C.; Ahn, D.; Shull, K. R. Macromolecules 2001, 34, 7448.
6. Flanigan, C. M.; Shull, K. R. Langmuir 1999, 15, 4966.
7. Shull, K. R.; Ahn, D.; Chen, W.-L.; Flanigan, C. M.; Crosby, A. J. Macromol Chem Phys 1998, 199, 489.
8. Creton, C.; Hooker, J. C.; Shull, K. R. Langmuir 2001, 16, 4948.
9. Chaudhury, M. K.; Weaver, T.; Hui, C. Y.; Kramer, E. J. J Appl Phys 1996, 80, 30.
10. Biot, M. A. J Appl Phys 1941, 12, 155.
11. Rice, J. R.; Cleary, M. P. Rev Geophys Space Phys 1976, 12, 227.
12. Chandler, R. N.; Johnson, D. L. J Appl Phys 1981, 52, 3391.
13. Biot, M. A. J Appl Phys 1962, 33, 1482.
14. Johnson, D. L. J Chem Phys 1982, 77, 1531.
15. Wang, H. F. Theory of Linear Poroelasticity with Applications to Geomechanics and Hydrogeology; Princeton University Press: Princeton, NJ, 2000.
16. Tanaka, T.; Hocker, L. O.; Benedek, G. B. J Chem Phys 1973, 59, 5151.
17. Johnson, K. L. Contact Mechanics; Cambridge University Press: Cambridge, UK, 1985.
18. Muskhelishvili, N. I. Some Basic Problems of the Mathematical Theory of Elasticity, 2nd ed.; Noordhoff International: Leyden, The Netherlands, 1977.
19. Geissler, E.; Hecht, A. M. J Chem Phys 1976, 65, 103.
20. Geissler, E.; Hecht, A. M. Polymer 1980, 21, 1358.
21. Geissler, E.; Hecht, A. M. Macromolecules 1980, 13, 1276.
22. Geissler, E.; Hecht, A. M. Macromolecules 1981, 14, 185.
23. Geissler, E.; Hecht, A. M.; Chosson, A. Polymer 1981, 22, 877.
24. Geissler, E.; Hecht, A. M. J Chem Phys 1982, 77, 1548.
25. Geissler, E.; Hecht, A. M. Polym Commun 1983, 24, 98.
26. Geissler, E.; Duplessix, R.; Hecht, A. M. Macromolecules 1983, 16, 712.